# Experimental investigation of the effect of middle ear in bone conduction

Dobrev, Ivo ; Farahmandi, Tahmine S ; Röösli, Christof

Abstract: Objectives: Experimental investigation of the contribution of the middle ear to bone conduction (BC) hearing sensation. Methods: Experiments were conducted on 6 fresh cadaver whole head specimens. The electromagnetic actuators from a commercial bone conduction hearing aid (BCHA), Baha® 5 SuperPower and BoneBridge (BB), were used to provide stepped sine stimulus in the range of 0.1-10 kHz. The middle ear transfer function (METF) of each cadaver head was checked against the ASTM F2504-05 standard. In a first step, the stapes stimulus into the cochlea, under BC, was estimated based on the differential velocity between the stapes footplate and the promontory. This was based on sequential measurements of the 3D velocity of the stapes footplate and the promontory. In parallel, the differential tympanic membrane (TM) pressure was recorded by measuring sound pressure in the middle ear and in the external auditory canal each measured 1-2 mm from the TM. The measurement procedure was then sequentially repeated, after: a) opening the middle ear cavity; b) ISJ interruption; c) closing the middle ear cavity. At the end, the velocity at each actuator is measured for comparison purposes. Stapes footplate and promontory motion was quantified as the 3D motion at a single measurement point via a three-dimensional laser Doppler vibrometer (3D LDV) system. The combined motion was used for all motion parameters. Results: The METF, based on the combined motion, matches better to the ASTM standard, making the measurements resilient to oblique measurement directions. The Baha actuator produced 10 dB SPL more output than the BB above 2 kHz. This resulted in 2-5 dB increase in the differential pressure across the TM, after middle ear cavity opening, for Baha stimulation, and up to 9 dB drop (around 2 kHz) for BB stimulation. The differential stapes motion follows linearly the level of motion of the stimulation area, however, it is affected by actuator resonances in a more complex way. Interruption of the ISJ, reduces the differential motion of the stapes with 1-5 dB, only at 1-3 kHz. Conclusion: Combined velocity more objectively describes the stapes and skull motion, than any individual motion component. The state of the ME cavity and the ISJ affect the cochlear input of the stapes, however, the effect is limited in frequency and magnitude.

DOI: https://doi.org/10.1016/j.heares.2020.108041

Dobrev, Ivo; Farahmandi, Tahmine S; Röösli, Christof (2020). Experimental investigation of the effect of middle ear in bone conduction. Hearing Research, 395:108041.
DOI: https://doi.org/10.1016/j.heares.2020.108041

Hearing Research 395 (2020) 108041

Contents lists available at ScienceDirect

Hearing Research

journal homepage: www.elsevier.com/locate/heares

Research Paper

# Experimental investigation of the effect of middle ear in bone conduction

Ivo Dobrev [a, b, *], Tahmine S. Farahmandi [a, b], Christof Röösli [a, b]

[a] Department of Otorhinolaryngology, Head and Neck Surgery, University Hospital Zürich, Zürich, Switzerland
[b] University of Zürich, Zürich, Switzerland

ARTICLE INFO

*Article history:*
Received 6 April 2020
Received in revised form
6 July 2020
Accepted 8 July 2020
Available online 30 July 2020

*Keywords:*
Bone conduction pathways
3D laser Doppler vibrometer
Middle ear
Cadaver head
Coupling condition

ABSTRACT

*Objectives:* Experimental investigation of the contribution of the middle ear to bone conduction (BC) hearing sensation.
*Methods:* Experiments were conducted on 6 fresh cadaver whole head specimens. The electromagnetic actuators from a commercial bone conduction hearing aid (BCHA), Baha® 5 SuperPower and BoneBridge (BB), were used to provide stepped sine stimulus in the range of 0.1−10 kHz. The middle ear transfer function (METF) of each cadaver head was checked against the ASTM F2504-05 standard. In a first step, the stapes stimulus into the cochlea, under BC, was estimated based on the differential velocity between the stapes footplate and the promontory. This was based on sequential measurements of the 3D velocity of the stapes footplate and the promontory. In parallel, the differential tympanic membrane (TM) pressure was recorded by measuring sound pressure in the middle ear and in the external auditory canal each measured 1−2 mm from the TM. The measurement procedure was then sequentially repeated, after: a) opening the middle ear cavity; b) ISJ interruption; c) closing the middle ear cavity. At the end, the velocity at each actuator is measured for comparison purposes. Stapes footplate and promontory motion was quantified as the 3D motion at a single measurement point via a three-dimensional laser Doppler vibrometer (3D LDV) system. The combined motion was used for all motion parameters.
*Results:* The METF, based on the combined motion, matches better to the ASTM standard, making the measurements resilient to oblique measurement directions. The Baha actuator produced ~10 dB SPL more output than the BB above 2 kHz. This resulted in 2−5 dB increase in the differential pressure across the TM, after middle ear cavity opening, for Baha stimulation, and up to 9 dB drop (around 2 kHz) for BB stimulation. The differential stapes motion follows linearly the level of motion of the stimulation area, however, it is affected by actuator resonances in a more complex way. Interruption of the ISJ, reduces the differential motion of the stapes with 1−5 dB, only at 1−3 kHz.
*Conclusion:* Combined velocity more objectively describes the stapes and skull motion, than any individual motion component. The state of the ME cavity and the ISJ affect the cochlear input of the stapes, however, the effect is limited in frequency and magnitude.


## 1. Introduction

Two different pathways exist of how sound reaches the inner ear. One way is air conduction (AC) stimulation that generates a sound pressure in the external auditory canal, which in turn induces vibration of the tympanic membrane. These vibrations are transmitted to the cochlea by the middle ear ossicles. The second pathway is bone conduction (BC). The pathways of sound transmission to the cochlea via BC is more complex and includes the following (Stenfelt, 2005): 1) sound radiation into the external auditory canal, 2) inertia of the middle ear ossicles, 3) inertia of the perilymph, 4) compression and expansion of the otic capsule, 5) sound pressure transmitted via the fluid pathways such as the cerebrospinal fluid via third windows (internal auditory canal, vestibular aqueduct). The contribution of these pathways is only partially understood. Determination of AC and BC is clinically used to distinguish conductive from sensorineural hearing loss. It is

* Corresponding author. Department of Otorhinolaryngology, Head and Neck Surgery, University Hospital Zürich, Frauenklinikstrasse 24, CH-8091, Zürich, Switzerland.
*E-mail address:* ivo.dobrev@usz.ch (I. Dobrev).

https://doi.org/10.1016/j.heares.2020.108041

assumed that BC represents inner ear function and AC both, inner and middle ear function. Therefore, it is expected that AC changes significantly in patients with conductive hearing loss whereas BC remains unchanged. However, in patients with a conductive hearing loss, BC shows a frequency dependent decrease mainly around 2 kHz. This finding is described as Carhart's notch in patients with otosclerosis and implies that BC pathways involving the ossicles may be important in pathologic situations (Carhart, 1971).

The first two BC pathways have in common that they stimulate the cochlea via the ossicles and a normal motion of the stapes footplate may be required for the third BC pathway. Previous studies showed that sound radiation into the external auditory canal is of minor importance. In a normal hearing population, umbo motion for AC and BC at hearing threshold was investigated (Röösli et al., 2012; Stenfelt, 2006). The two studies showed larger ossicular motion for AC stimulation compared to BC stimulation at hearing threshold at 3 kHz and below, indicating that ossicular motion elicited by BC is not sufficient to induce cochlear activation. At frequencies above 3 kHz, ossicular motion for BC stimulation were larger than for AC stimulation at hearing threshold. Therefore, a hearing sensation via ossicular activation was assumed. However, sound radiated from the BC stimulator into the non-occluded external auditory canal could be responsible for this observation.

It is challenging to distinguish between middle and inner ear inertia experimentally (BC pathway 2 and 3). In a computational model, it was shown that inner ear inertia is dominant for almost the entire frequency range of 0.1–10 kHz (Stenfelt, 2016). Inner ear compression and middle ear inertia were within 10 dB for almost the entire frequency range. It was confirmed that ear canal sound pressure contributed little at the low and high frequencies, but was around 15 dB below the total contribution at mid frequencies. Assuming that the impedance of the oval window limits the contribution of inner ear inertia, it could be assumed that stapes footplate motion increases after transection of the incudostapedial joint. This increase in stapes footplate motion should be measurable by Laser Doppler Vibrometry (LDV). Therefore, the aim of this study was to experimentally investigate the contribution of the middle ear to BC hearing in normal situation and in case of an interrupted ossicular chain.

## 2. Methods

### 2.1. Measurement procedure

First, the middle ear transfer function (METF), under AC stimulation, was quantified as the ratio of the stapes motion to the driving acoustic pressure at the tympanic membrane (TM). This was done by simultaneously measuring the velocity of the stapes footplate and differential pressure across the TM. The differential TM pressure was quantified based on acoustic pressure measurements in the ear canal and middle ear cavity, each measured at distance of 1–2 mm away from the lateral and medial surface of the TM, respectively. Measurements under acoustic excitation were conducted with an acoustically sealed middle ear and ear canal. The ear canal was sealed with a foam tip of the speaker deeply inserted to about 5 mm from the tympanic membrane. This allowed for the quantification of the METF checking its compliance with the American Society for Testing and Materials (ASTM) standard (F2504-05, Philadelphia, 2005). After AC stimulation testing, the following measurement steps were performed sequentially, all under BC stimulation:

1) In a 1st step, the stapes stimulus into the cochlea, under BC, was estimated based on the differential velocity between the stapes footplate and the promontory. This was based on sequential measurements of the 3D velocity of the stapes footplate and the promontory. In parallel, the differential TM pressure was as in the METF measurements. Stimulation is applied consequently with two commercial actuators – one percutaneous and subcutaneous. This is referred to as condition 1, where the middle ear is considered intact.
2) In a 2nd step, the middle ear cavity is opened, and measurement procedure of step 1 is repeated. This is referred to as condition 2.
3) In a 3rd step, the ISJ is interrupted and measurement procedure of step 1 is repeated. This is referred to as condition 3.
4) In a 4th step, the middle ear cavity is closed, and measurement procedure of step 1 is repeated. This is referred to as condition 4.
5) At the end, the velocity at each actuator is measured for comparison purposes.

### 2.2. Sample preparation

This study was approved by the Ethical Committee of Zürich (KEK-ZH-Nr. 2012–0136) and was conducted experimentally in 6 fresh human cadaver heads acquired from Science Care (Phoenix, Arizona, USA). The specimens were in the age range of 56–89 years (6 males). The cadaver heads were originally frozen and were defrosted 1 day before the experiment. In order to verify the thawing of the contents of the head, the temperature was checked in the nasal cavity and middle ear with a thermal probe. In order to provide an optical access to stapes footplate and promontory, an anterior mastoidectomy was performed. The facial nerve and the chorda tympani were identified and a wide posterior tympanotomy was opened by removing the bone between the nerves as well as the facial nerve in the mastoidal segment. This allowed a clear identification of all three ossicles. In order to acoustically seal the middle ear cavity, while maintaining the optical access to the middle ear, the lateral opening of the mastoidectomy at the level of the cortical bone was blocked with a transparent glass with anti-reflective coating (WG11010-A, Thorlabs, NJ, USA), mechanically held with malleable putty (Play-Doh©, Cincinnati, Ohio, USA) and acoustically sealed with Vaseline, as seen in Fig. 1. This allowed for the precise repositioning of the glass (based on the imprint of the glass in the putty), when closing back the middle ear cavity, resulting in a middle ear cavity pressure repeatability of approximately 1 dB, based on preliminary tests.

BC stimulation was provided by the actuators of a Baha 5 SuperPower (referred to as Baha) (Cochlear Company, Australia) and BoneBridge (referred to as BB) (BCI 601 actuator, MED-EL, Austria), both modified to allow direct driving via an audio power amplifier. For coupling of the Baha actuator via Baha Connect, a BI300 was implanted at the classical BAHA location, 5 cm posterior and slightly superior to the external auditory canal. The BB actuator was implanted into the cortex of the mastoid bone, by drilling a well of 16 mm diameter and 9 mm depth, between the posterior edge of the mastoidectomy and the sigmoid sinus (Huber et al., 2013). Subsequently, the device was fixed to the skull bone with two titanium self-tapping cortex screws with a length of 6 mm and an external diameter of 2 mm. The skull surface area at the implants was left exposed for optical access to the contact area of each actuator. The heads were supported in a natural upright position via a custom head support, as shown in Fig. 2. Details on the head support assembly as well as discussions on its potential benefits are presented in previous publications (Dobrev et al., 2019, 2020).

In order to quantify the velocity at the output of each bone conduction hearing aid (BCHA) actuator, the area (<1 $mm^2$) at the connection of each device with the skull was carefully cleaned and covered with retroreflective beads (30–100 μm in diameter, P2453BTA-4.2 30–100 μm, Cospheric LLC, CA, USA) for better signal

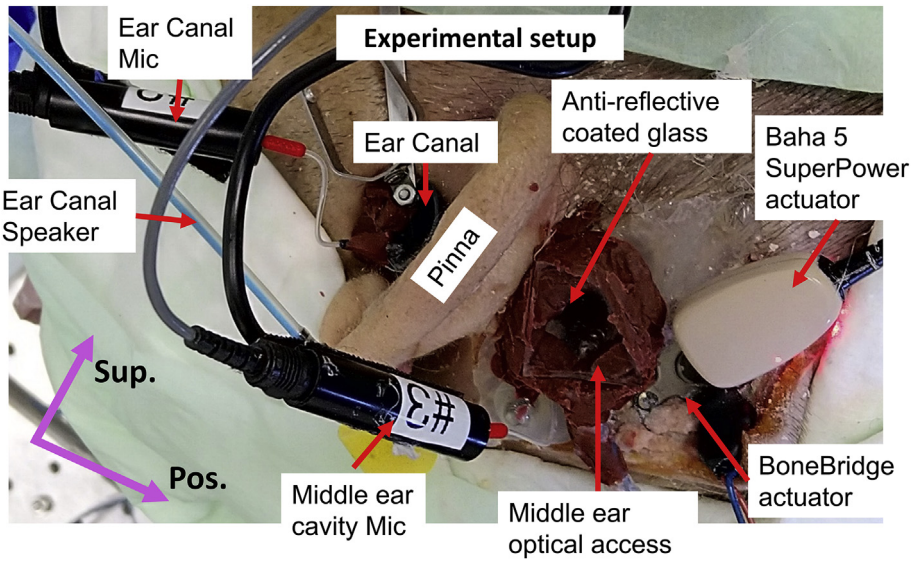


**Fig. 1.** Overview of experimental setup. Indicated are the middle ear optical access for 3D LDV measurements of the velocity promontory and stapes, microphones for monitoring acoustic pressure in the outer and middle ear, as well as BCHA actuators for BC stimulation.

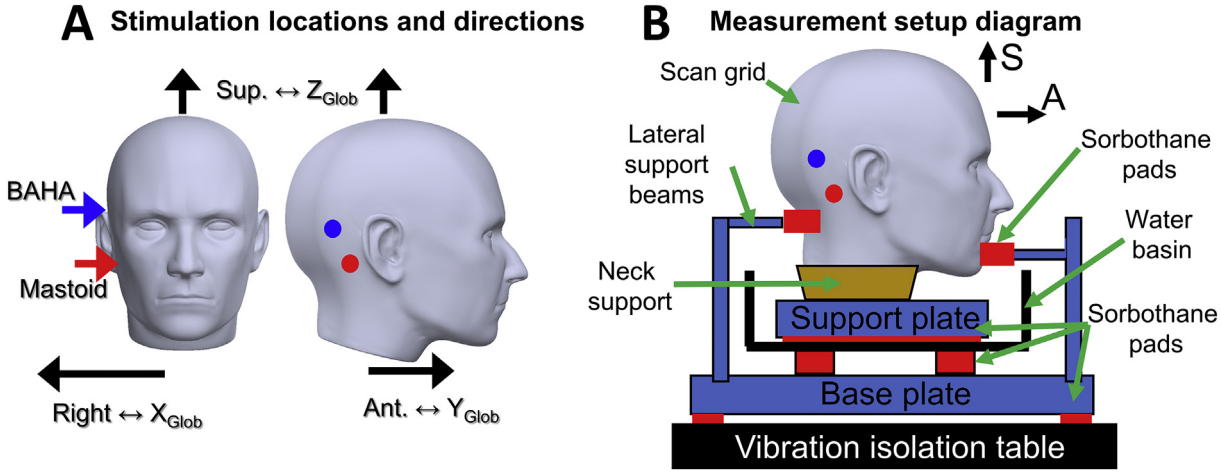


**Fig. 2.** Overview of: A) stimulation direction and location; B) custom head support. Noted is the correspondence between the anatomical direction and the global (Glob) coordinate system used for data representation. Abbreviations: Ant. is anterior; Sup. is superior.

quality of the three-dimensional laser Doppler vibrometer (3D LDV) system. In the case of the Baha actuator, measurements were done at the rim of the BI300 implant, immediately (<0.5 mm) lateral from the surface of the skull, as shown in Fig. 3A. In the case of the BB, the velocity response of 3 points on the actuator, shown in Fig. 3B, were measured: 1) one point near the center of lateral wall (near the skull surface) of the body actuator, where the actuator mechanism is housed; 2) 1 point on each of the attachment screws connecting the actuator wings to the skull.

In order to quantify the velocity of the stapes and footplate, a small area (<0.5 $mm^2$) was carefully cleaned and covered with retroreflective beads (30–100 μm in diameter, P2453BTA-4.2 30–100 μm, Cospheric LLC, CA, USA) for better signal with the 3D LDV system. Approximate locations of the velocity measurement for the promontory and footplate are indicated in Fig. 4. In order to monitor the differential pressure across the tympanic membrane (TM) two microphones (ER-7C, Etymotic Research, USA) were installed, one in the middle ear cavity and one in the external ear canal. The microphone in the ear canal was held in a constant position via an otoscope speculum (4 mm, HEINE Optotechnik, Germany) tightly inserted into the ear canal. A speaker (ER-2, Etymotic Research, USA) was also inserted into the ear canal through the otoscope speculum, such that it could be removed during BC stimulation, without changing the position of the ear canal microphone. After initial set of measurements, the incudo-stapedial joint was interrupted with a diode laser (Ceralas, Biolitec, Germany), as seen in Fig. 4. Care was taken to create a visible gap between incus and stapes. The laser beam was aimed slightly lateral from the incudo-stapedial joint, in order to primarily ablate the lenticular process of the incus and reduce damage to the stapes head, and the overall stapes mechanics. A manual palpation was performed at the end of the procedure, in order to verify stapes mobility.

### 2.3. Data acquisition

Both actuators provided a stepped sine stimulus in the range of 0.1–10 kHz. A total of 100 stimulus frequencies were used,

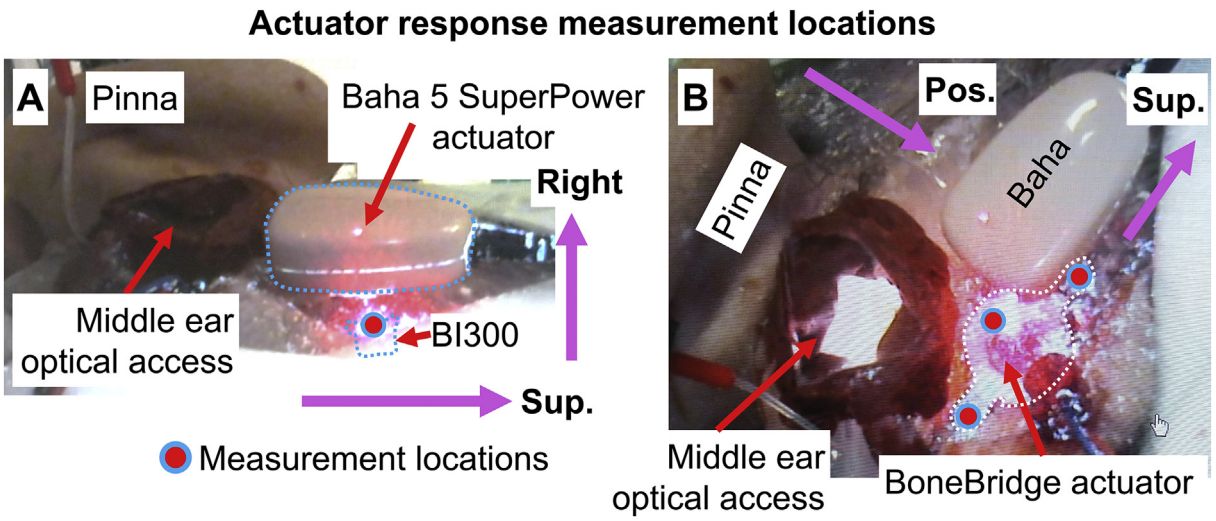


**Fig. 3.** Illustration of the measurement locations and direction for quantification of the vibrations at the output of the BCHA actuator: A) Baha 5 SuperPower attached at the BAHA location via a BI300 implant; B) BB secured at the mastoid via 2 self-cutting screws. Images are from the perspective of the 3D LDV system, along its optical (Z) axis.

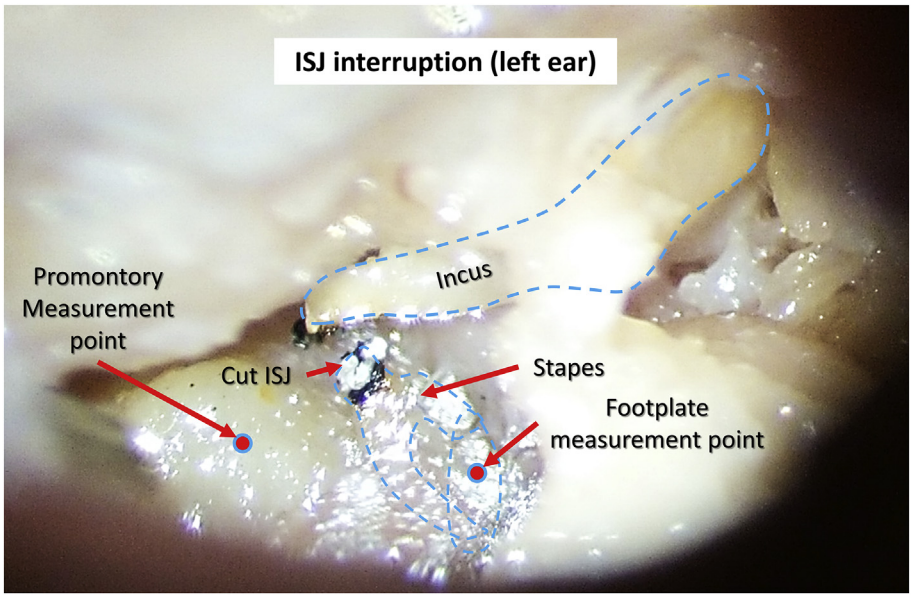


**Fig. 4.** Microscope view of the incudo-stapedial joint after interruption by ablation with a surgical laser. The stapes and incus are outlined for clarity. The approximate locations of the velocity measurements on the stapes footplate and the promontory are indicated.

distributed linearly in 100 Hz increments. The actuators were modified to allow for direct electrical stimulation from the analog output of a data acquisition device (DAQ) (NI-4431, National Instruments, USA) via an audio amplifier (RMX 850a, QSC, CA, USA). The stimulus at each frequency was presented continuously for 200 ms with a sinusoidal-shaped ramp up (onset) region of 20 ms and a constant stimulation voltage of 0.3 Vrms, for both actuators.

The stimulus was provided 5 consecutive times (iterations) per frequency for averaging purposes. The measurement procedure was repeated sequentially for measurement condition and stimulation device, resulting in ~3–4 h for all measurements per sample. The signal generation, motion response recoding and overall automation was handled via a custom-made MATLAB script (MATLAB, 2018a; MathWorks, MA, USA). Each stimulus tone was digitally synthesized as a sinusoidal waveform and output via the analog output channel of the DAQ at 192 kS/s and 24 bit of temporal and amplitude resolution, respectively.

The velocity at each measurement point was quantified along 3 orthogonal directions via a three-dimensional laser Doppler vibrometer (3D LDV) system (3D CLV 3000, Polytec, Germany). The unique position and orientation of the 3D LDV at each measurement location was controlled and monitored via a robotic arm (KR 16, KUKA, Germany). The orientation of the optical axis (Z axis) of 3D LDV was visually adjusted to be approximately normal to the skull surface. Exception was the measurements of the BI300, where the Baha Superpower actuator body was obstructing optical axis in the normal direction. In this case, the 3D LDV was oriented approximately tangent to the skull surface (as seen in Fig. 3 A), such that the Y-axis of the 3D LDV was oriented along the surface normal. Final representation of the 3D velocity accounted for this difference in orientation and reports all velocity components in the same frame of reference.

### 2.4. Data analysis and representation

At each measurement point, all three Cartesian components of the velocity were measured, and the combined velocity, $\mathbf{V_{COMB}}$, was calculated based on methods described previously (Dobrev et al., 2017; Dobrev and Sim, 2018). The $\mathbf{V_{COMB}}$ is calculated as the maximum of the instantaneous vector sum of all 3 orthogonal velocity components, such that it accounts for not only their magnitudes, but also their phase and direction. From a physiological perspective, the combined velocity, $\mathbf{V_{COMB}}$, is indicative of the total vibratory motion and it corresponds total kinetic energy at a given measurement point, regardless of measurement direction and coordinate system (Dobrev and Sim, 2018; Stenfelt and Goode, 2005a, 2005b). In addition, the combined velocity of the promontory has been observed to be a better representation of the perceived sound (i.e., closer to hearing sensation), compared to any of the individual components alone (Stenfelt and Goode, 2005b; Dobrev and Sim, 2018).

The 3D LDV optical axis (z-axis) was approximately at 45–60 deg to the stapes footplate normal (piston) direction, with the X-Z plane of the 3D LDV, being coplanar with the plane of the normal and long axis (skull horizontal), and the Y-axis pointing along the short axis of the footplate (Sim et al., 2010). This meant that the piston component of the motion of the stapes was sensed by the X and Z axis of the 3D LDV. While the volume displacement of the piston motion component is a good estimator of hearing sensation (Eiber et al., 2012), estimation of the volume displacement from a single point measurement is reasonable up to 2–3 kHz, beyond which the stapes undergoes complex spatio-temporal vibration modes. This is complicated even further, when the rigid body motion of the footplate needs to be estimated relative to the motion of the surrounding bone. Based on that, and due to time limitations with the duration of each experiment relative to the temporal stability of the samples, the combined velocity, $\mathbf{V_{COMB}}$, was used to approximate the motion of the stapes and the promontory, without any further spatial corrections (transformations).

In order to estimate the response of the stapes footplate for every measurement condition, its velocity vector, $\mathbf{V_{FOOTPLATE}}$, was normalized relative to the promontory velocity vector, $\mathbf{V_{PROMONTORY}}$, resulting in a metrics (also a vector) called differential velocity vector, $\mathbf{V_{DIFF}}$, similar to the "differential relative velocity" used by Stenfelt et al. (2002):

$$\vec{V}_{Diff} = \frac{\vec{V}_{Footplate} - \vec{V}_{Promontory}}{\left|\vec{V}_{Promotory\_combined}\right|}$$

The numerator represents the vector difference (3 components) between the velocity vectors of the stapes, $\mathbf{V_{Footplate}}$, and the promontory, $\mathbf{V_{Promontory}}$. The denominator is the magnitude of the combined motion of the promontory velocity vector, used for scaling of the metrics relative to the otic capsule motion, represented by the promontory motion. All calculations were done with the complex values of the velocity. The differential velocity, $\mathbf{V_{DIFF}}$, is a metrics quantifying the amount of relative 3D motion between the stapes and the promontory, normalized by the magnitude of the promontory 3D motion (indicative of the input). The differential velocity of the stapes gives an indication of the scala vestibuli activation. It should be noted that this metrics does not indicate the direction of the power, e.g. from middle-ear to cochlea or vice versa. The differential velocity under BC stimulation is analogical to the definition of the middle-ear transfer function under AC stimulation, where stapes motion is normalized to ear-canal pressure (the input). While the metrics have 3 complex components, each with a magnitude and phase, further analysis in this work have been based on the magnitude of combined differential velocity vector. A value of 0 for the combined $\mathbf{V_{DIFF}}$ indicates no relative motion between the stapes and the cochlea in any direction. A value of 1 indicates a differential stapes velocity equivalent to the promontory velocity. Any value between 0 and 1, indicates differential motion less than the promontory motion, and vice versa for values above 1.

## 3. Results

### 3.1. METF compliance with ASTM

The middle ear transfer function (METF) for AC stimulation of all samples (N = 6) was calculated based on the orthogonal components $V_X$, $V_Y$, and $V_Z$, defined within the 3D LDV coordinate system. In addition, the combined velocity $\mathbf{V_{COMB}}$ of the stapes footplate motion was also calculated and used for calculation of the METF. The AC stimulus acoustic pressure in the ear canal was 90–105 dB SPL >500 Hz for all samples.

The METF was compared against the ASTM standard 2504–05 for normal footplate motion. Sample 1's METF was more than 10 dB above the upper bound of the 95% confidence interval of the ASTM standard, while sample 3 was 5 dB below the lower bound, for all frequencies. The remaining 4 samples were used to plot the METF mean and confidence interval as shown in Fig. 5. The METF based on the X and Z components, showed a close match to the ASTM, above 1,5 kHz, and approximately 10 dB lower response at lower frequencies. This is consistent with the fact that both the X and Z components are sensitive to the stapes piston component of motion. The METF based on the Y component showed 10–20 dB lower response below 4 kHz. The mean of the METF, based on the combined motion, was within the ASTM confidence interval for nearly all frequencies, except at 400 Hz and 6–8 kHz. Based on the observations in Fig. 5, the combined motion was used as metrics for calculation of the differential velocity in the rest of this work.

### 3.2. Differential pressure across TM under bone conduction

Estimation of the acoustic stimulus to the middle ear, under BC, was done based on the difference of the acoustic pressures measured in the ear canal and the middle ear, defined as differential pressure across the TM. This metrics was quantified for each measurement condition and stimulation device, as shown in Fig. 6 A and E. In addition, the change in the differential pressure, for each measurement condition (conditions 2–4), was expressed as the magnitude of the complex ratio of each specific differential pressure to the initial one for the intact ear (condition 1), as shown in Fig. 6 B-D and F–H. A 95% confidence interval is estimated and plotted only for frequencies, where at least 3 samples had valid data, thus the confidence interval (CI) is not shown for all frequencies below 0.5 kHz in panels B–D and F–H. This is mainly due to the low response of the samples as a result of the low stimulus level from the BC actuators at those frequencies. Since samples 1 and 3 did not exhibit normal METF, they were excluded from the data in Fig. 6. Based on data in Fig. 6 A and E, both BB and Baha actuators induced 60–90 dB SPL differential pressure above 500 Hz, with the Baha producing ~10 dB SPL more than the BB actuator above 2 kHz. Opening of the middle ear cavity (condition 2) resulted in 5–10 dB drop in the differential pressure at 0.5–4 kHz, particularly at 2 kHz, for BB stimulation, as seen in Figure Fig. 6 B. In contrast, with Baha stimulation there was a 2–5 dB increase in the differential pressure in the same frequency range, as seen in Fig. 6F. However, this increase had a local minimum (1–3 dB lower than nearby values) at 2 kHz, qualitatively similar to the data in Fig. 6B.

Interrupting the ISJ, while keeping the ME cavity open (Fig. 6 C and G), produced a change in the differential pressure, relative to

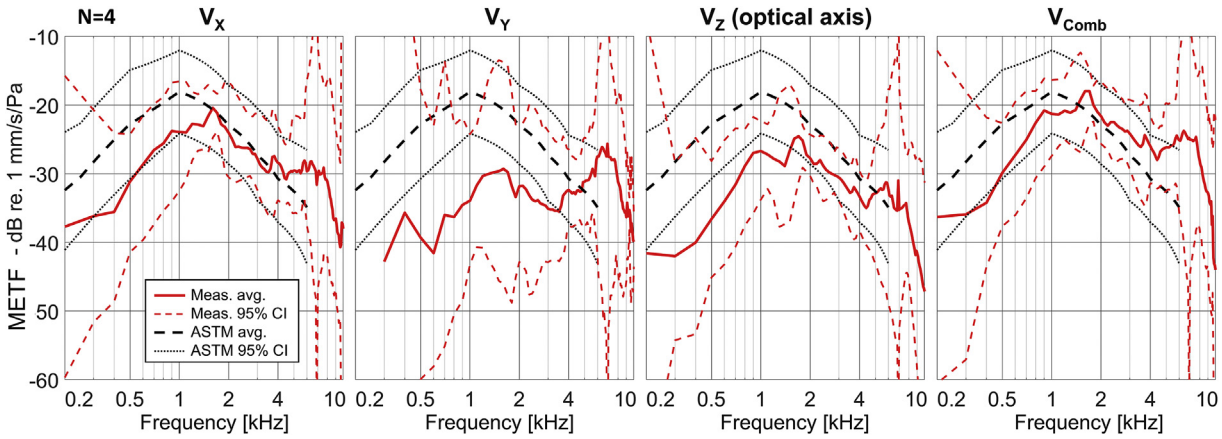


**Fig. 5.** Middle ear transfer function (METF) for AC stimulation, based on the orthogonal components $\mathbf{V_X}$, $\mathbf{V_Y}$, $\mathbf{V_Z}$ and the combined velocity $\mathbf{V_{COMB}}$ of the stapes footplate motion, and the differential pressure across the TM (N = 4). Red lines indicate average (thick solid lines) and 95% confidence interval (CI) bounds (thin dashed lines) of the measured METF. Black lines indicate the average (thick dashed lines) and 95% CI bounds (thin dotted lines) of the ASTM standard 2504–05 for METF. . (For interpretation of the references to color in this figure legend, the reader is referred to the Web version of this article.)

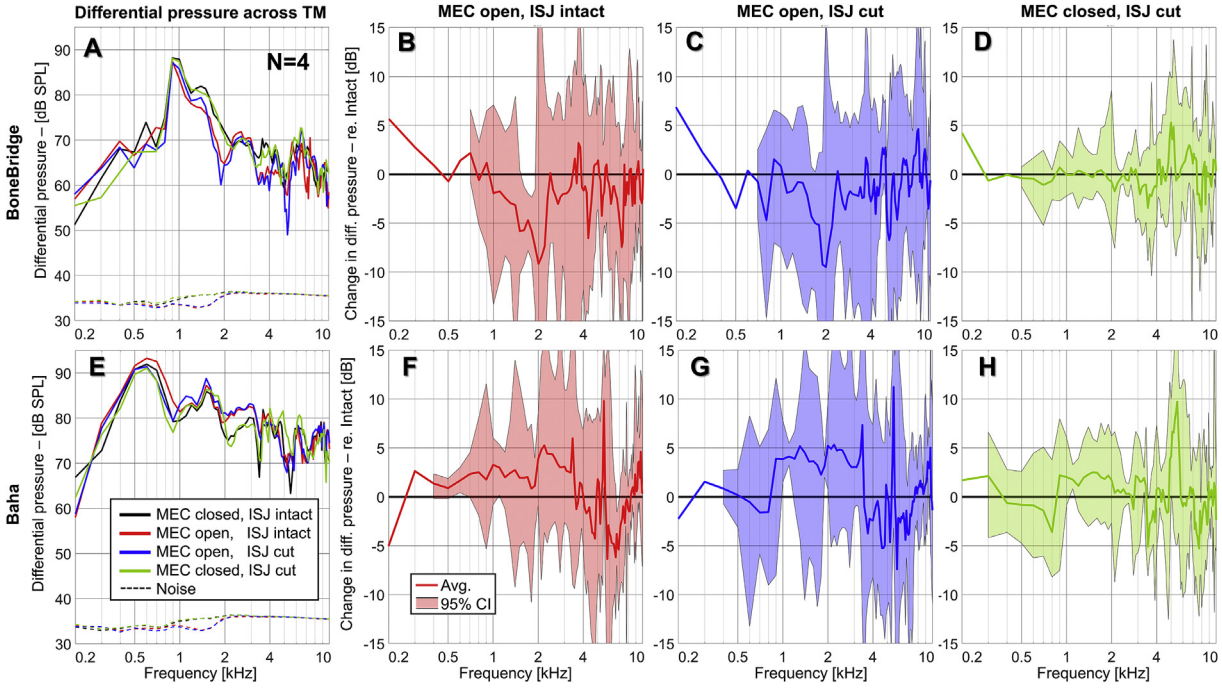


**Fig. 6.** The differential pressure (A and E) across the TM for BC and the change (ratio) in the differential pressure due to MEC opening and ISJ interruption, relative to the intact ear (N = 4): B-D) for stimulation with BB; F–H) for stimulation with Baha. Both actuators were driven with constant 0.3 Vrms. Each line is an average of the response of 4 samples. Noise floor in A and E) is shown with dashed lines. A 95% confidence interval (CI) is shown in B-D and F–H with colored bands around each average line. MEC is middle ear cavity, ISJ is incudo-stapedial joint.

condition 2 (MEC open, Fig. 6 B and F), that was consistent with both BB and Baha stimulation. Namely 1–2 dB decrease at 300–900 Hz, and 1–2 dB increase at 1–1.5 kHz, with qualitative similarities at higher frequencies as well. For BB stimulation, closing the ME cavity, with interrupted ISJ (Fig. 6 D), approximately restored the differential pressure to its original levels at 0.5–4 kHz, increased it with 1–4 dB at 4–7 kHz, and decreased it with 1–3 dB above 7 kHz. For Baha stimulation (Fig. 6 H), the ME cavity closure had a similar effect on the differential pressure as with BB stimulation, however, the restoring effect at the mid frequencies was limited and a 1–2 dB shift from the intact condition remained.

### 3.3. Comparison of the device and skull response

Data in Fig. 7 A shows the combined velocity response of the Baha, measured at the lateral rim of the BI300, as illustrated in Fig. 3 A. The response is compared to the response at 3 points on the BB, as illustrated in Fig. 3 B. Fig. 7 B highlights the differences in the velocity output of the two devices, by taking the ratio of the BB versus the Baha. It can be seen that the BB velocity output is 5–25 dB lower across all frequencies, and specifically 15–25 dB lower <500 Hz, 5–15 dB lower at 1–6 kHz, and 15–20 dB lower above 6 kHz. The central section of the body of the BB moves 2–7 dB faster than the wings. The two wings have similar motion

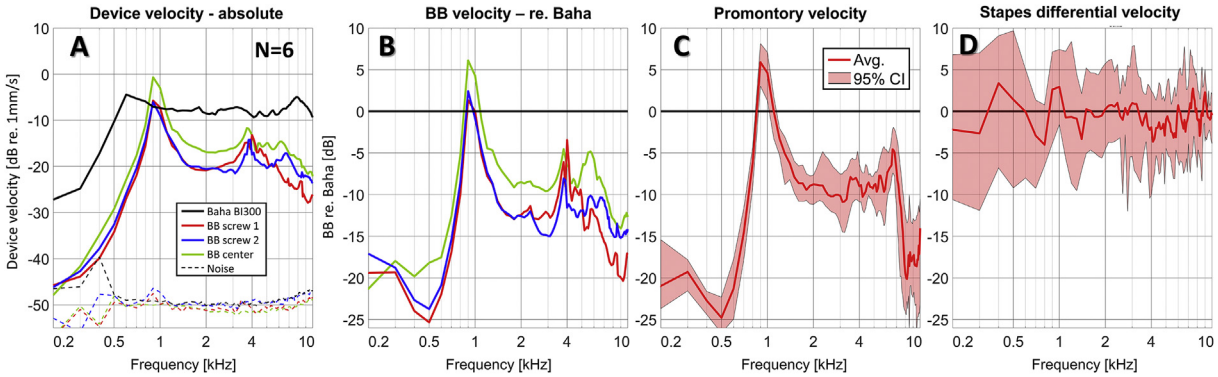


**Fig. 7.** Comparison of the combined motion of the device, the promontory and the differential stapes motion, for the Baha Power and BB actuators (N = 6): A) magnitude of the combined velocity for each measurement point at the actuators; B) velocity ratio of the BB relative to the Baha 5 SuperPower; C) Promontory motion for stimulation with BB relative to Baha 5 SuperPower; D) Differential stapes motion for stimulation with BB relative to Baha 5 SuperPower. Both actuators were driven with constant 0.3 Vrms. The Baha Power velocity (black line in A and B) was measured at the lateral rim of the BI300. The BB output was measured at the metal housing of the center (green line) of the body of the actuator, and at the screws (red and blue lines in A and B) holding the wings. Each line is an average of the response of 6 samples. Noise floor in A) is shown with dashed lines. A 95% confidence interval (CI) is shown in C and D with colored bands around each average line. BB is BoneBridge. . (For interpretation of the references to color in this figure legend, the reader is referred to the Web version of this article.)

up to 2 kHz, and differences of 2–5 dB at higher frequencies.

Fig. 7 C, shows the difference in promontory motion between the two actuators, similar to Fig. 7 B. The drop in the promontory motion, for BB relative to Baha, approximately follows the average of the drop of the response of all 3 points on the BB body, relative to the Baha, as seen in Fig. 7 B. The differential motion of the stapes relative to the promontory, indicated in Fig. 7 D, for BB stimulation is within −2 to 1 dB of that for Baha stimulation, across all frequencies. An exception is a 1–3 dB drop at 4–6 kHz relative to the Baha stimulation. In this range, the BB exhibits a resonance (Fig. 7 A and B) that is not seen in the promontory motion (Fig. 7 C).

### 3.4. Relative motion between stapes and promontory

In order to quantify the effect of interrupting the ISJ and opening the ME on the differential motion between the stapes and the promontory, the change in differential motion of the stapes was compared in each of the 4 conditions, as shown in Fig. 8. Data for sample 1 was excluded from the analysis in Fig. 8, because of qualitative difference in its behavior, due to ME changes, relative to the other samples. However, sample 3 was included in Fig. 8, even though it showed lower METF.

Under all conditions, the differential motion of the stapes, relative to the promontory, was approximately −25 dB at 200 Hz, and it increased up to approximately 5 dB at 3 kHz, at a rate of approximately 25–30 dB/decade. At higher frequencies, the differential motion remained at 0 dB, meaning the difference between the stapes and promontory motions was as much as the promontory motion itself. Opening the ME cavity (Fig. 8 A) increased the differential motion with 1–3 dB for all frequencies. Interrupting the ISJ (Fig. 8 B), while the ME cavity is open, resulted in 2–6 dB drop <2 kHz, and 1–3 dB increase at higher frequencies. Closing the ME cavity (Fig. 8 C), while the ISJ is interrupted, resulted in a 1–4 dB increase across all frequencies, similar to the inverse effect the data in Fig. 8 A. Interrupting the ISJ (Fig. 8 D), while the ME cavity is closed, resulted in 1–7 dB drop < 2 kHz, and no change at higher frequencies. This effect was similar for stimulation with BB, as shown in Fig. 8 E, with the exception of frequencies above 8 kHz, where there was a drop of 2–8 dB.

Since the promontory motion was measured multiple times, in order to reference the stapes motion against it, it was used to monitor any shifts in the response of the head or the actuators. The difference between the first and the last promontory motion, with either actuator, was limited to within 1 dB.

## 4. Discussion

### 4.1. METF compliance with ASTM standard

The use of the combined velocity for the estimation of the METF, under AC stimulation, allowed for more accurate assessment of the stapes motion as has been demonstrated before (Dobrev and Sim, 2018; Dobrev et al., 2019). This was especially helpful with the current surgical access to the footplate, which resulted in 45–60 degree of inclination of the optical axis of the 3D LDV relative to the piston direction of the stapes footplate (i.e., surface normal). Using only the velocity component along the optical axis ($V_Z$) of the 3D LDV would have resulted in 10–15 dB underestimation of the stapes footplate response, as demonstrated by comparing Fig. 5 C and D. In order words, the METF, based on the combined motion, matches better to the ASTM standard, making the measurements insensitive to the oblique measurement direction. In addition, due to the complex spatio-temporal vibration modes of the rigid body motion of the stapes footplate (Sim et al., 2010) above 2–3 kHz, all motion components contribute nearly equally to the motion of each point at the footplate. While not all samples (4 out of 6) complied with the ASTM for METF, all samples were used in the rest of the analysis, as device or promontory motion data was not affected by potential pathologies in the middle ear.

### 4.2. Effects on TM differential pressure

The effect of opening the ME cavity on the differential pressure across the TM, under BC stimulation, differed between the two actuators. While stimulation with both devices resulted in no change on average above 4 kHz, there was approximately 2–4 dB drop at 1–3 kHz for BoneBridge (BB) stimulation, but a 1–3 dB increase at the same frequencies for Baha stimulation. Disrupting the ISJ, while keeping the ME cavity open, had negligible effect on the differential pressure for both stimulation methods. Finally, closing the ME cavity, after the ISJ interruption, resulted in approximately restoring the differential pressure to its original levels, on average across all frequencies. There was a tendency for an increase of 1–2 dB at 1–4 kHz for Baha stimulation, but this was not seen in data with BB stimulation. This could be related to a difference in the amount of acoustic emissions from the two

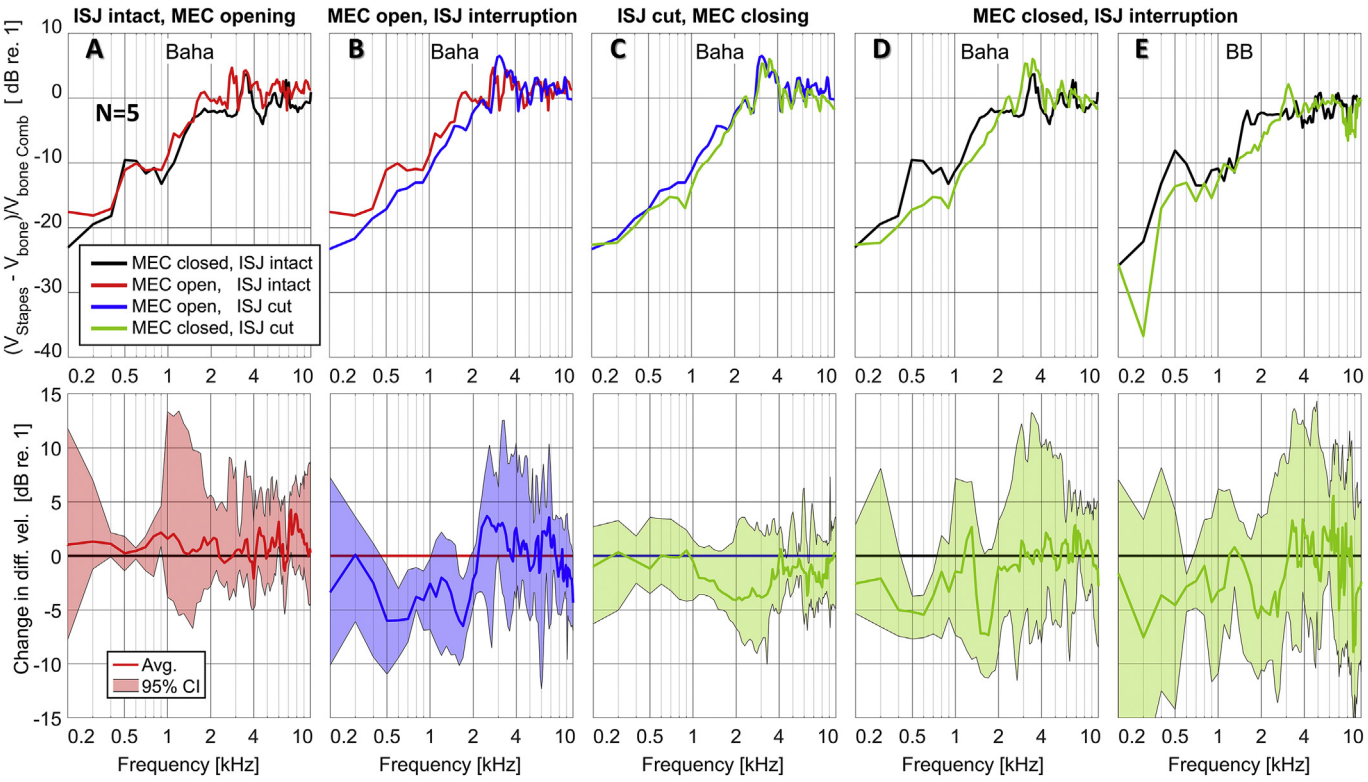


**Fig. 8.** The effect of interrupting the ISJ and opening the ME to the differential motion between the stapes and the promontory, for Baha and BB stimulation (N = 5). The conditions, under Baha 5 SuperPower stimulation, include the effect of: A) Opening the ME cavity; B) interruption of the ISJ, while the ME cavity is open; C) Closing the ME, while the ISJ is interrupted; D) interruption of the ISJ, while the ME cavity is closed; E) same as D) but with BB stimulation. Each line is an average of the response of 5 samples. A 95% confidence interval (CI) is shown in bottom row of panels with colored bands around each average line. BB is BoneBridge, MEC is middle ear cavity, ISJ is incudo-stapedial joint.

devices (Carlsson, 1990; Akhshijan, 2011; Huber et al., 2013), due to their different function and implantation method. In particular, the BB is fully embedded in the skull bone, with only exposure of its lateral surface to skin and connecting tissue, while the Baha has its entire surface exposed to air.

It is hypothesized that three main pathways play are role in the mechanism of middle ear activation under BC stimulation, and each pathway has different contribution relative from the output of each actuator. One potential pathway is the inertial loading of the cochlea fluid, which in turn could drive the middle ear "in reverse" (Stieger et al., 2013; Ravicz et al., 2019), through the stapes, resulting in differential pressure across the TM and differential stapes motion. A second potential pathway is the inertial loading of the ossicles, due to ME cavity wall vibrations, causing relative motion between the ossicles and the cavity walls. This pathway could have a similar effect on the TM differential pressure as the first pathway, however the driving source in this case are all support structures of the ME, rather than the stapes alone. Another possible pathway is the direct air-conducted sound emitted from the actuator, which could drive the TM via differential pressure, since the ear canal is open.

With this hypothesis in mind, the differences between the BB and Baha stimulation could be explained as follows. Opening the ME cavity has the effect of reducing its acoustic impedance (Voss et al., 2000), which in turn provides lower resistance to the motion of the TM, driven by BC, thus reducing the differential pressure across it. This effect has been also seen under AC, where an increase in the TM surface motion has been observed with opening the ME cavity (Tang et al., 2019). This effect seems to be particularly strong around 2 kHz, exhibiting an "anti-resonance" in the differential pressure with opening the ME cavity. This effect will be present with both Baha and BB stimulation. However, since the Baha stimulation has a strong AC pathway (Akhshijan, 2011), opening the ME cavity could also have a 2nd effect, which will tend to increase the differential pressure across the TM. Namely, the opening will provide a direct AC pathway into the middle ear, due to its closer vicinity to the Baha actuator, relative to the ear canal. It seems that the strength of this 2nd effect, under Baha stimulation, overpowers the effect of the "anti-resonance" from the ME cavity opening, resulting in the total increase in the differential pressure. Resealing the ME cavity, reduces the strength of the air conducted pathway under the Baha stimulus, reducing the differential pressure. However, the ISJ interruption could be reducing the overall ME impedance, causing an increase in differential pressure due to the residual AC stimulation via the open ear canal, under Baha stimulation. The combined effect of these two opposing effects, for Baha stimulation, is the resultant increase in differential pressure after ISJ interruption and resealing of the ME cavity (Fig. 6H). In contrast, under BB stimulation, the ISJ interruption does not affect significantly the relevant dynamics of the TM, potentially the main differential pressure generator in the ME cavity. In order words, under BB stimulation, there is less contribution from the AC pathway, relative to the influence of the BC pathway common to both actuators. It should be noted that there could be differences in the inertial loading by the BC pathway of each device, causing differences in the spatial composition of the relative motion of the middle ear and the ME cavity walls. Further investigation of the spatial motion of the ossicles (Dobrev et al., 2016), could give a better understanding and differentiation between the various mechanisms of the ME excitation under BC.

It should be noted that the differential pressure under AC stimulus was 90–110 dB SPL in comparison to 70–90 dB SPL under

BC stimulus. This discrepancy is potentially due to differences between umbo velocity and ear canal pressure under BC stimulation (Reinfeldt et al., 2013; Röösli et al., 2012). This results in typically lower ear canal pressure below 2 kHz (Röösli et al., 2012). Thus, direct comparison based only on the generated ear-canal pressure between the two stimulation conditions is difficult. However, data in the current study have shown that stapes motion, above 1–2 kHz, would be equivalent to 80–100 dB SPL ear canal pressure, if the stapes footplate would have moved that much under acoustic stimulation. In addition, Stieger et al. (2018) have indicated comparable differential pressures across the cochlear partition, between an AC stimulation with 100 dB SPL and BC stimulation with 0.1–1mm/s in temporal bones. These bone motion levels are similar to the ones reported here.

It should be noted that the average 95% confidence interval of the intersample variability of the differential pressure data, shown in Fig. 6, was in the range of 2–10 dB. Thus, the small changes (1–3 dB) in the average differential pressure at any frequency should be interpreted with care.

### 4.3. Relation between device output and skull response

By comparing the data in panels B and C of Fig. 7, it can be observed that differences in the velocity response at the anchor points of the two devices propagate themselves into nearly identical differences in the resulting promontory motion. In this case, the motion is expressed as the combined velocity, making the magnitude estimates insensitive to the differences in the measurement direction, and more relevant to the underlying sound energy transfer, than any single motion component. This is supported by observations in several previous studies (Stenfelt and Goode, 2005b; Dobrev et al., 2017, Dobrev and Sim, 2018, Dobrev at al. 2020), indicating that above 1 kHz (transition frequency of the skull), the skull undergoes vibrational motion with nearly equal contributions from all motion components, regardless of stimulation location, coupling or device. This is also supported by the 3D velocity data that was used to calculate the combined motion of the device velocity in Fig. 7A, where, above the first natural frequency of each device, there was less than 5 dB difference between any of the orthogonal motion components. Thus above 1 kHz, the frequency dependence of the measured acoustic pressures or velocities are mostly influenced by differences (unique for each device type, coupling, and stimulation location) in transmitted total power (Stenfelt and Goode, 2005b) via each possible pathway (see section 4.2) from the device to each of the major functional structures of the ear. It should be noted that below 1 kHz, the skull could follow the primary stimulation direction of the actuator, however, other motion components are typically within 5–10 dB of the “main” direction, particularly for stimulation near the base of the skull (e.g., mastoid, BAHA location). It should be also noted that the relation between velocity at the stimulation area and force input into the skull could be different between actuators, thus velocity only measurements do not fully describe the power flow from the actuator to the ear.

However, in the case of the BB stimulation, there is uncertainty about which point (i.e., anchor screws versus body center) on the actuator body is representative of the velocity of the contact area. This could be due to the uncertainty in the contact area between the BB and the skull bone, which could be affected by potential resonance modes of the BB actuator body. Particularly, the resonances at around 4 kHz (peaks in panels A and B of Fig. 7), measured on the BB body and wings, were not observed as differences in the promontory motion between the two devices (panel C on Fig. 7). In other words, differences in the velocity of the BB, due to device’s resonances, seemed to not affect the promontory motion, as these could be spatially localized only on the device itself. In addition, based on data in panels C and D on Fig. 7, while there is 10–20 dB difference in the promontory motion level between the two devices, the corresponding difference in the differential stapes velocity is limited to −4 to 3 dB, with approximately no average difference across all frequencies. This is indicative of the linearity of the ratio between the differential stapes motion and actuator output velocity (near stimulation area). In other words, the stapes response relative to promontory seems to be independent of stimulation level. Again, an exception is the 3–6 kHz band of resonances at the BB, where there was a 1–4 dB drop in the differential stapes velocity induced by the BB, relative to the corresponding response under Baha stimulation. It should be noted that at low frequencies (<700 Hz) the BB provided 10–25 dB lower stimulation than the Baha, for the same stimulation voltage, thus differences in the results between the two devices at those frequencies should be interpreted with case.

It should also be noted that different coupling and stimulation positions, as well as the effect of the mastoidectomy, might induce some unforeseen uncertainties. The BB is about 3–4 cm away from the ear canal, while the Baha is about 5 cm away. This difference in the distance to the ear could induce 2–10 dB difference in the promontory response between the two devices, based on the stimulation location alone (based on analogy with I-3 and I-2 locations on the occiput, in Stenfelt and Goode, 2005b). The effect of the mastoidectomy could be estimated based on results from Dobrev et al. (2018), where it was shown that mastoidectomy has little effect on the promontory response for stimulation at the BAHA location, however, it could change (−15 to +5 dB) the response for stimulation near (<1 cm) the mastoidectomy. Specifically, increasing the mid-frequencies, and decreasing the high-frequency response, making it similar to one with stimulation at the BAHA location. Current methods in this work partially account for differences on the simulation level by normalizing stapes motion to the promontory motion. This normalization, however, does not account for potential changes in the direction or composition of the rigid body motion of the stapes, due to changes in the spatio-temporal characteristics of the stimulation, which could result in different cochlea stimulation from the middle ear.

### 4.4. Effect of middle ear on stapes motion

Under all conditions, the differential motion of the stapes (Fig. 8), relative to the promontory, exhibited a resonant frequency at around 3 kHz, where the differential motion exceeded the promontory motion, while at higher frequencies the differential motion was approximately as much as the promontory motion. At frequencies below the resonance, the differential motion decreased with decreasing frequency at a rate similar to data in literature from equivalent measurements in temporal bones (Stenfelt, 2006; Stenfelt et al., 2002). It should be noted that in data sets, the slopes were steeper (35–40dB/decade versus 25–30dB/decade in the current study) and the resonance frequency was an octave lower. However, the temporal bones were stimulated in a specialized manner to achieve a purer motion (less contribution from other components) along the stimulation direction, which differs from the complex spatial vibration response of the cadaver heads. The smaller mass of the temporal bone relative to the intact heads and the shaker could have had an influence on the resonance frequency as well as the spatial composition of the differential stapes motion, due to the “purer” stimulus. Regardless of methodological differences with previous work, the effects of the low frequency behavior (below the first resonance) of the differential motion of the stapes, and its influence on the cochlea activation in particular, have been observed in the relation between promontory motion and scala

vestibuli pressure in human temporal bones (Stieger et al., 2018) as well as correlation between promontory motion and hearing sensation in patients (Eeg-Olofsson et al., 2013). Namely, the scala vestibuli pressure and hearing sensation have been observed to be low relative to the measurement promontory motion at low frequencies, as expected from the low differential motion of the stapes below the first resonance frequency, as seen throughout the top row of panels in Fig. 8. This general behavior (both below and above the resonant frequency) remained approximately the same (within ±5 dB), regardless of the state of the middle ear cavity (i.e., open or close, Fig. 8A and C) or the ISJ (i.e., intact or interrupted, Fig. 8B and D), or type of BC stimulus (Fig. 8D and E).

The effect of opening the ME (column A in Fig. 8) was overall positive for the differential stapes motion, with approximately 1–4 dB increase across all frequencies, particularly > 4 kHz. This could be attributed to the increased contribution from the AC stimulation pathway, resulting in increased differential pressure in Fig. 6 D, as discussed in Section 4.2.

Interrupting the ISJ (column B in Fig. 8) seems to negatively affect frequencies below 2 kHz, and positively affect higher frequencies. The change in the differential stapes motion, with ISJ separation and closed ME, is similar for both actuators (Fig. 8D and E), even though the AC pathway for the Baha might have been stronger and it should have been influenced more by the ISJ interruption, than under BB stimulation. A potential explanation could be that the AC pathway is stronger through the ME cavity opening than through the ear canal, since the cavity is much (2–3x) closer to the actuators. Thus, since this acoustic pathway is blocked (or at least reduced) with closing the cavity, there is less of an influence from the ISJ interruption on the differential stapes motion from the remaining AC pathway through the ear canal.

The frequency profile of the change in the differential stapes motion, due to ISJ interruption, is qualitatively similar to previous measurements by Stenfelt et al. (2002). Namely, a mild (1–5 dB) drop below 1 kHz, and a more significant drop (2–7 dB) at 1–2 kHz. However, the Stenfelt et al. (2002) study showed stronger drop of up to 10–11 dB, affecting frequencies up to 3–4 kHz, which was not observed to this extend in this current work. Qualitatively similar influence of the IS joint interruption on differential cochlea pressure, under bone conduction, was observed in temporal bones of rodents (Chhan et al., 2013) and humans (Stieger et al., 2015). Any quantitative differences could be due to differences in methodology, such as measurement of a single component along the piston direction of the stapes versus the combined motion measured in this study. In addition, there is no primary excitation direction in this study, as there is approximately equal contribution from all motion components above 1 kHz, as seen previously (Stenfelt and Goode, 2005b; Dobrev et al., 2017, 2019; 2020; Dobrev and Sim, 2018), while the stimulation in Stenfelt et al. (2002) was primarily (within 15–20 dB, up to 5–6 kHz) in a direction along the piston direction of the footplate. However, both data suggest that the influence of the middle ear to the differential stapes motion (and the corresponding cochlea activation) is frequency limited to < 2–3 kHz.

Closing of the ME cavity (column C in Fig. 8) appears to negate the high and low frequency effect of the ISJ interruption, leaving only the 1–5 dB drop of differential motion < 4 kHz, particularly around 2 kHz. This general effect appears consistent in stimulation with either device. This could be contributed to a resonance of the ME, which could be affecting (increasing) the differential motion of the stapes, under intact condition, and disappearing with ISJ separation. In other words, under BC stimulation, the ME resonance had a considerable effect on the differential motion of the stapes around 2 kHz.

While, the differential motion in piston direction could be approximately estimated in the current data set and in Stenfelt et al. (2002), the resulting volume displacement of the stapes, cannot be defined based on single point measurement (Sim et al., 2010). This is especially relevant in pathological and implanted ears. More accurate estimation of the middle ear contribution to the cochlea activation could be achieved by estimating the volume velocity at the footplate, relative to the promontory (Stenfelt and Goode, 2005a). However, this requires the measurement of the motion and location of several points across the footplate, in order to estimate of the piston component of the rigid body motion of the footplate (Sim et al., 2010; Eiber et al., 2012).

In addition, it has been shown that promontory motion alone may not concur to scala vestibuli pressure at all frequencies (Borgers et al., 2019), thus differential stapes motion was used in this study. Both Grossöhmichen et al. (2016) and Stieger et al. (2018) have indicated an approximately flat (at low and mid frequencies) relation between scala vestibuli pressure and stapes motion, under AC stimulation, of around 10–100 Pa/mm/s (scala vestibuli pressure versus footplate motion). However, under BC stimulation Stieger et al. (2018) have indicated similar values, when comparing scala vestibuli pressure to promontory motion (not normalization with stapes motion), only at mid and high frequencies, while observing a 20–30dB/decade decrease with decreasing frequencies below 1.5 kHz. This is also supported by data from Eeg-Olofsson et al. (2013), showing good correlation between promontory motion and hearing sensation in patients only above 1 kHz, but not below. This correlates well with data in Fig. 8, where the stapes motion followed the promontory motion below 2 kHz, resulting in small differential motion, in contrast to the behavior at higher frequencies. This suggests that differential stapes motion, rather than promontory motion alone, could be a good indicator of scala vestibuli pressure. However, more detailed examination of the correlation between middle ear motion and cochlea activation should include cochlea pressure measurements (Grossöhmichen et al., 2016; Stieger et al., 2018; Borgers et al., 2019).

## 5. Conclusions

Combined velocity more objectively describes the stapes and skull motion, than any individual motion component. The state of the ME cavity and the ISJ affect the cochlear input of the stapes, however, the effect is limited in frequency and magnitude.

## CRediT authorship contribution statement

**Ivo Dobrev:** Conceptualization, Methodology, Formal analysis, Writing - original draft, Data curation, Visualization. **Tahmine S. Farahmandi:** Data curation, Formal analysis, Writing - original draft. **Christof Röösli:** Conceptualization, Methodology, Writing - review & editing, Supervision, Project administration, Funding acquisition.

## Acknowledgements

This work was supported by Swiss National Foundation Grant 325230-166377.

## Appendix A. Supplementary data

Supplementary data to this article can be found online at https://doi.org/10.1016/j.heares.2020.108041.

## References


Akhshijan, S.S., 2011. Feedback Analysis in Bone Anchored Hearing Aid (BAHA) and Bone Conduction Implant (BCI) (Master's thesis). Department of Signal and System, Division of Signal Processing and Biomedical Engineering, Chalmers University of Technology.

Borgers, C., Fierens, G., Putzeys, T., van Wieringen, A., Verhaert, N., 2019. Reducing artifacts in intracochlear pressure measurements to study sound transmission by bone conduction stimulation in humans. Otol. Neurotol. 40 (9), e858–e867.

Carhart, R., 1971. Effects of stapes fixation on bone-conduction response. In: Ventry, I., Chaiklin, J., Dixon, R. (Eds.), Hearing Measurement: A Book of Readings. Appleton,Century, Crofts, New York, pp. 116–129.

Carlsson, P.U., 1990. On Direct Bone Conduction Hearing Devices: Advances in Transducer Technology and Measurement Methods. Ph.D. thesis. School of Electrical and Computer Engineering, Chalmers University of Technology. isbn 0282-5406.

Chhan, D., Röösli, C., McKinnon, M.L., Rosowski, J.J., 2013. Evidence of inner ear contribution in bone conduction in chinchilla. Hear. Res. 301, 66–71.

Dobrev, I., Farahmandi, T., Sim, J.H., Pfiffner, F., Huber, A.M., Röösli, C., 2020. Dependence of skull surface wave propagation on stimulation sites and direction under bone conduction. J. Acoust. Soc. Am. 147 (3), 1985.

Dobrev, I., Sim, J.H., Pfiffner, F., Huber, A.M., Röösli, C., 2019. Experimental investigation of promontory motion and intracranial pressure following bone conduction: stimulation site and coupling type dependence. Hear. Res. 378, 108–125.

Dobrev, I., Sim, J.H., 2018. Magnitude and phase of three-dimensional (3D) velocity vector: application to measurement of cochlear promontory motion during bone conduction sound transmission. Hear. Res. 364, 96–103.

Dobrev, I., Sim, J.H., Pfiffner, F., Huber, A.M., Röösli, C., 2018. Performance evaluation of a novel piezoelectric subcutaneous bone conduction device. Hear. Res. 370, 94–104.

Dobrev, I., Sim, J.H., Stenfelt, S., Ihrle, S., Gerig, R., Pfiffner, F., Eiber, A., Huber, A.M., Röösli, C., 2017. Sound wave propagation on the human skull surface with bone conduction stimulation. Hear. Res. 355, 1–13.

Dobrev, I., Ihrle, S., Röösli, C., Gerig, R., Eiber, A., Huber, A.M., Sim, J.H., 2016. A method to measure sound transmission via the malleus–incus complex. Hear. Res. 340, 89–98.

Eeg-Olofsson, M., Stenfelt, S., Taghavi, H., Reinfeldt, S., Håkansson, B., Tengstrand, T., Finizia, C., 2013. Transmission of bone conducted sound–correlation between hearing perception and cochlear vibration. Hear. Res. 306, 11–20.

Eiber, A., Huber, A.M., Lauxmann, M., Chatzimichalis, M., Sequeira, D., Sim, J.H., 2012. Contribution of complex stapes motion to cochlea activation. Hear. Res. 284 (1–2), 82–92.

Grossöhmichen, M., Salcher, R., Püschel, K., Lenarz, T., Maier, H., 2016. Differential Intracochlear Sound Pressure Measurements in Human Temporal Bones with an Off-The-Shelf Sensor. BioMed research international, 2016.

Huber, A.M., Sim, J.H., Xie, Y.Z., Chatzimichalis, M., Ullrich, O., Röösli, C., 2013. The Bonebridge: preclinical evaluation of a new transcutaneously-activated bone anchored hearing device. Hear. Res. 301, 93–99.

Ravicz, M.E., Cheng, J.T., Rosowski, J.J., 2019. Sound pressure distribution within human ear canals: II. Reverse mechanical stimulation. J. Acoust. Soc. Am. 145 (3), 1569–1583.

Röösli, C., Chhan, D., Halpin, C., Rosowski, J.J., 2012. Comparison of umbo velocity in air- and bone-conduction. Hear. Res. 290 (1–2), 83–90.

Reinfeldt, S., Stenfelt, S., Håkansson, B., 2013. Estimation of bone conduction skull transmission by hearing thresholds and ear-canal sound pressure. Hear. Res. 299, 19–28.

Sim, J.H., Chatzimichalis, M., Lauxmann, M., Röösli, C., Eiber, A., Huber, A.M., 2010. Complex stapes motions in human ears. Journal of the Association for Research in Otolaryngology 11 (3), 329–341.

Stenfelt, S., Hato, N., Goode, R.L., 2002. Factors contributing to bone conduction: the middle ear. J. Acoust. Soc. Am. 111 (2), 947–959.

Stenfelt, S., 2006. Middle ear ossicles motion at hearing thresholds with air conduction and bone conduction stimulation. J. Acoust. Soc. Am. 119 (5 Pt 1), 2848–2858.

Stenfelt, S., 2016. Model predictions for bone conduction perception in the human. Hear. Res. 340, 135–143.

Stenfelt, S., Goode, R.L., 2005a. Bone-conducted sound: physiological and clinical aspects. Otol. Neurotol. 26 (6), 1245–1261.

Stenfelt, S., Goode, R.L., 2005b. Transmission properties of bone conducted sound: measurements in cadaver heads. J. Acoust. Soc. Am. 118 (4), 2373–2391.

Stieger, C., Rosowski, J.J., Nakajima, H.H., 2013. Comparison of forward (ear-canal) and reverse (round-window) sound stimulation of the cochlea. Hear. Res. 301, 105–114.

Stieger, C., Farahmand, R.B., Page, B.F., Roushan, K., Merchant, J.P., Abur, D., Rosowski, J.J., Nakajima, H.H., 2015. December. Pressures in the human cochlea during bone conduction. In: AIP Conference Proceedings, vol. 1703. AIP Publishing LLC. No. 1, p. 060004.

Stieger, C., Guan, X., Farahmand, R.B., Page, B.F., Merchant, J.P., Abur, D., Nakajima, H.H., 2018. Intracochlear sound pressure measurements in normal human temporal bones during bone conduction stimulation. Journal of the Association for Research in Otolaryngology 19 (5), 523–539.

Tang, H., Razavi, P., Pooladvand, K., Psota, P., Maftoon, N., Rosowski, J.J., Furlong, C., Cheng, J.T., 2019. High-speed holographic shape and full-field displacement measurements of the tympanic membrane in normal and experimentally simulated pathological ears. Appl. Sci. 9 (14), 2809.

Voss, S.E., Rosowski, J.J., Merchant, S.N., Peake, W.T., 2000. Acoustic responses of the human middle ear. Hear. Res. 150 (1–2), 43–69.